Journal of the European Ceramic Society **5** (1989) 11–22

The Control of Morphology in Silicon Nitride Powder Prepared from Rice Husk

I. A. Rahman & F. L. Riley*

Division of Ceramics, School of Materials, University of Leeds, Leeds LS2 9JT, UK

(Received 3 December 1987; accepted 18 April 1988)

Abstract

α-Silicon nitride powder of high purity has been prepared by nitriding pyrolysed rice husk at temperatures between 1260 and 1450°C under 95% nitrogen–5% hydrogen. Hydrogen addition is beneficial in accelerating the rate of nitride formation. The addition of iron (III) oxide and nickel (II) oxide to the rice husk promotes the competitive formation of silicon carbide at temperature as low as 1300°C. Other transition metal oxides are without catalytic effect on the nitridation reaction, though vanadium (V) oxide favours formation of β-phase silicon nitride. The silicon nitride particle morphology is determined in part by the particle dimension of the milled rice husk. Silicon nitride crystals of hexagonal symmetry are obtained from starting powder of dimension ≤53 μm, whereas greater particle dimensions, and lower packing densities, yield silicon nitride of a whiskery morphology. Addition of pre-formed silicon nitride powder results in the formation of fine, equiaxed, silicon nitride particles.

α-Siliziumnitrid von hoher Reinheit wurde durch Nitridierung von pyrolysierten Reishülsen bei Temperaturen zwischen 1260 und 1450°C unter einer Stickstoff–Wasserstoffatmosphäre (95:5 Vol.%) hergestellt. Eine Wasserstoffzugabe beschleunigt die Bildungsrate der Nitridierung. Die Zugabe von Eisen(III)-Oxid und Nickel (II)-Oxid zu den Reishülsen fördert die konkurrierende Bildung von SiC bei Temperaturen bis herab zu 1300°C. Andere Übergangsmetalloxide sind ohne katalytischen Einfluß auf die Nitridierung, wobei Vanadium(V)-Oxid die Bildung von β-Si_3N_4 fördert. Die Siliziumnitrid–Teilchenmorphologie wird durch die Partikelgröße der gemahlenen Reishülsen bestimmt. Si_3N_4 mit hexagonaler Symmetrie wird aus Ausgangspulvern mit Teilchengrößen ≤ 53 μm erhalten; größere Teilchenabmessungen und geringere Packungsdichten führen zu Siliziumnitrid mit Whiskermorphologie. Die Zugabe von bereits gebildeten Si_3N_4 resultiert in der Bildung feiner äquiaxialer Si_3N_4-Teilchen.

Une poudre de nitrure de silicium α de haute pureté a été préparée par nitruration de balles de riz pyrolysées à des températures comprises entre 1260 et 1450°C dans un mélange contenant 95% d'azote et 5% d'hydrogène. L'addition d'hydrogène augmente la vitesse de formation du nitrure. L'addition d'oxyde de fer (III) et d'oxyde de nickel (II) aux balles de riz favorise la formation concurrente de carbure de silicium à une température de 1300°C. Les autres oxydes des métaux de transition n'ont pas d'effet catalytique sur la réaction de nitruration, bien que l'oxyde de vanadium (V) favorise la formation du nitrure de silicium β. La morphologie des particules de nitrure de silicium est déterminée en partie par la dimension des particules de balles de riz broyées. On obtient des cristaux de nitrure de silicium de symétrie hexgonale à partir d'une poudre de départ de taille ≤53 μm, alors qu'une granulométrie de départ supérieure et des densités tassées inférieurs produisent un nitrure de silicium possédant une morphologie proche de celle des whiskers. L'addition d'une poudre de nitrure de silicium aux réactifs provoque la formation de particules de nitrure de silicium fines et isotropes.

1 Introduction

Silicon nitride powder may be produced in a number of ways.[1] The oldest established method is the reaction of elemental silicon and nitrogen.[2] The

* To whom all correspondence should be addressed.

Journal of the European Ceramic Society 0955-2219/89/$3.50

process is slow, varying proportion of α- and β-phase silicon nitride are produced, the silicon nitride particles tend to be agglomerated and milling is required to produce a sinterable powder. A higher purity, predominantly α-phase silicon nitride powder is obtained by the simultaneous reduction and nitridation of silicon dioxide powder by carbon in the presence of nitrogen (carbothermal reduction), a potentially attractive route because of the availability and low cost of the raw materials.[3-9] This process constitutes an alternative large-scale production method for silicon nitride powder and has the further merit that finer particle sizes can readily be produced. A third series of routes uses chemical reactions of, for example, the silicon halides to produce silicon nitride powder of very high purity and high specific surface area. This type of powder is likely to be relatively expensive.[1]

One aim of the present work was to investigate the possibility of producing a high quality sinterable silicon nitride powder from Malaysian rice husk. A study of the carbothermal reduction process was extended to include the addition of metal oxides as potential catalysts for the process. Identification of catalysts able to accelerate the rate of formation of silicon nitride was seen as attractive, and it would also be potentially advantageous to incorporate metal oxide sintering aids into the silicon nitride at this stage. These studies led to an investigation of the use of pre-formed silicon nitride powder as an additive for the nitridation step.

Rice husk, a by-product of the paddy mill, is a unique agricultural waste. Although the main components of rice husk are organic materials, they produce on oxidation a large amount of ash which comprises 13–29 mass % of the husk, depending on the variety, climate and geographical location.[10] The ash is largely composed of silicon dioxide (87–97 mass %) with metallic oxide impurity. Carbonization, or pyrolysis of the husk (by heating in an atmosphere of low oxygen content) produces an intimate mixture of carbon and silicon dioxide. This high carbon ash can be used to prepare either silicon nitride or silicon carbide, according to the conditions. The synthesis of silicon carbide from rice husk has been studied in detail.[11-13] The feasibility of the production of silicon nitride was reported by Hanna *et al.*[14] and by Kang and Chun,[15] but the latter study concentrated only on the effect of iron as a reaction catalyst. The introduction of iron can result in silicon nitride powder containing silicon carbide impurity.[14,16]

The carbothermal reduction and nitridation of silicon dioxide is normally carried out at temperatures below 1450°C and in the presence of excess carbon, in order to obtain a reasonable reaction rate and to ensure a minimal residue of oxygen. At higher temperatures, silicon nitride in the presence of carbon tends to become unstable with respect to silicon carbide. The overall nitridation reaction equation for this process may be written:

$$3SiO_{2(s)} + 6C_{(s)} + 2N_{2(g)} \rightarrow Si_3N_{4(s)} + 6CO_{(g)} \quad (1)$$

Because two solid reactants are involved, a high powder surface area and homogeneous particle distribution is normally advantageous. In the case of the use of rice husk as the simultaneous source both of carbon and silicon dioxide, these requirements are met naturally.

2 Experimental

Rice husk was washed three times with deionized water and dried at 100°C for 10 ks. The dried husk was pyrolysed at 700°C for 2 ks under a flow of argon (1·5 $cm^3 s^{-1}$). Pyrolysed rice husk (PRH) was crushed in a tungsten carbide lined mill (Shatter Box—Glen Creston, Stanmore, UK) to provide the starting powders for nitridation (PRH powder).

PRH powder was boiled in 0·3 M hydrochloric acid for 7 ks in order to leach out as much metallic contamination as possible. It was then filtered and washed repeatedly with warm, deionized water until free from chloride, as shown by the absence of visible reaction of the wash water with $AgNO_3$ solution, and dried. Chemical analysis of combusted, purified PRH powder was carried out using dilute hydrofluoric acid solution, by atomic absorption spectrophotometry. The carbon content of PRH powder was determined by heating at 700°C in air to constant mass. The mass loss after heating was considered to be the mass of carbon present in the PRH powder.

A range of different particle sizes of PRH powder was prepared by crushing 20 g batches in the tungsten carbide mill for 3 s. The resulting powder was sieved using No. 44, 72 and 300 mesh sieves (BS 410 Test Sieves, London) with apertures corresponding to 350, 210 and 53 μm respectively. The powder was again leached with 0·3 M hydrochloric acid as described above. To determine tap densities, dry powder was poured into a 25 ml measuring cylinder and vibrated electrically for 30 s. Surface area determinations of silicon nitride powders were carried out using a single point BET method (Perkin Elmer Adsorptometer).

The possible effects of a number of additives on

the nitridation behaviour of the PRH powder were examined. These materials were added to the PRH powder by wet mixing in water for 40 ks followed by spray drying (Buchi 190, Switzerland). Materials incorporated (based on the silicon dioxide equivalent of the PRH powder) are listed in Table 1. The effect of added preformed silicon nitride ('LC 10', H. C. Starck, Berlin) on nitridation was also investigated. This silicon nitride was incorporated by wet mixing and spray drying as above. In the following discussions materials are designated, for example, as PRH–$2Al_2O_3$, indicating PRH powder incorporating 2 mass % aluminium oxide.

Small scale nitridation experiments were first carried out in a controlled atmosphere platinum resistance furnace. Approximately 1·5 g of PRH contained in a graphite boat was heated at 1260–1500°C for times up to 30 ks using a controlled gas flow rate. Preliminary studies showed that nitridation was significantly faster in 95% nitrogen–5% hydrogen than in 100% nitrogen, and this gas mixture was used in all subsequent work. Silicon nitride was produced on a larger scale in a silicon carbide resistance furnace. After nitridation excess carbon was burned off in flowing air at 690°C over 14 ks.

Nitrogen analyses of the nitrided materials were carried out by alkali fusion and acid–base titration.[17] Accurately weighed ~0·1 g portions were fused with 10 g sodium hydroxide (99·8% Analar Grade, BDH, Poole, Dorset, UK) in a thick-walled pyrex tube. The ammonia evolved was collected in 200 ml of 2 mass % boric acid solution using a slow stream of argon as carrier gas. The resulting solution was titrated with standard hydrochloric acid solution (0·1M) against a mixed indicator (bromo-cresol green and methyl red). The analyses were later checked by a CHN-Analyser (M1106, Carlo Elba, Italy), where nitrogen and carbon were analysed simultaneously. The agreement between the two methods was ~0·5%. Nitrogen contents (f_N) are expressed as percent of the theoretical value for silicon nitride of 39·94 mass %. In cases where silicon carbide was formed, the carbon content (f_C) is expressed as percent of the theoretical value for silicon carbide of 29·95 mass%.

X-Ray diffraction (XRD) analyses of nitrided products were carried out using Ni-filtered CuK α radiation (40 kV, 20 mA). The examination was made between $2\phi = 12$ to 60° with a scanning speed of 1° min^{-1}. The XRD intensities of selected strong peaks for α-Si_3N_4 (210), β-Si_3N_4 (200), Si_2N_2O (200) and β-SiC (111) were obtained and phase compositions were calculated using the standard method described elsewhere.[18]

Scanning electron (SEM) micrographs were obtained using an Hitachi S700 microscope (Hitachi, Tokyo). A small quantity of powder was dispersed in acetone and the dispersion was dropped on a glass-covered 12 mm aluminium stub. After drying the specimen was coated with a thin film of gold, or with carbon, when energy dispersion X-ray analyses (EDAX) were to be carried out.

Table 1. Materials incorporated into PRH powder

	Purity (mass %)	*Amount added (mass % based on SiO_2 in PRH)*
Group 1		
Aluminium oxide	97	2
Yttrium oxide	99·9	2
Zirconium (IV) oxide	99	5
Group 2		
Titanium (IV) oxide	99	5
Cerium (IV) oxide	99·95	5
Group 3		
Iron (III) oxide	98·5	2
Nickel (II) oxide	98·5	2
Group 4		
Vanadium (V) oxide	99	2
Other ('seed')		
Silicon nitride ($\alpha/\beta = 16$, ~0·3 μm)	Starck LC10	10

3 Results

Table 2 shows the chemical composition of rice husk ash after washing with 0·3 M hydrochloric acid. Figure 1 illustrates the effect of temperature on the pyrolysis of rice husk under argon atmosphere (flow rate = 1·5 cm^{-3} s^{-1}) for a time of 2 ks. At a temperature of ~700°C most of the volatile organic material was removed, leaving ~60 mass % of carbonaceous material. This PRH powder had a carbon to silicon dioxide molar ratio of ~7 (mass ratio ~1·5). Scanning electron micrographs of rice husk after pyrolysing and milling are shown in

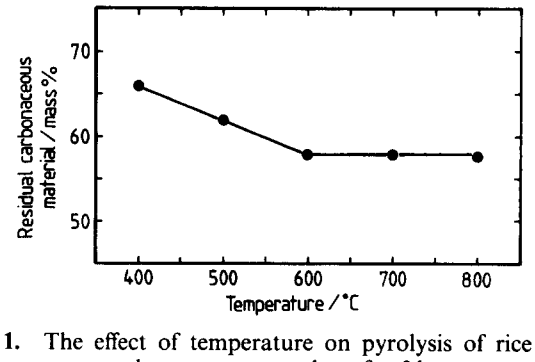

Fig. 1. The effect of temperature on pyrolysis of rice husk under argon atmosphere for 2 ks.

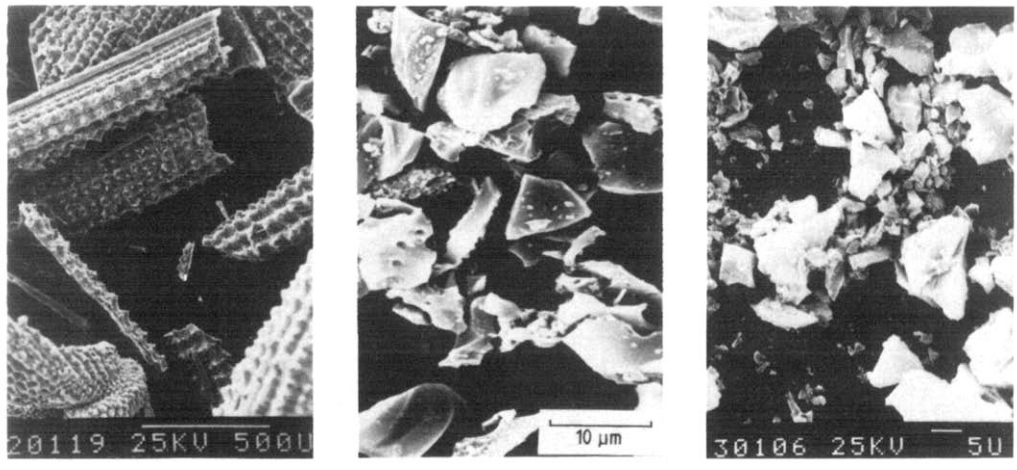

(a) (b) (c)

Fig. 2. SEM of rice husk (a) pyrolysed at 700°C, (b) milled for 90 s, (c) milled for 1·8 ks.

Fig. 2. An attempt was made to measure the specific surface area of PRH powder, but this was not successful, possibly due to the highly porous nature of the material (see Fig. 2). The effect of gas flow rate on the nitridation of PRH powder at 1400°C for a time of 7 ks is shown in Fig. 3. The optimum flow rate was found to be ~ 17 cm^3 s^{-1}. This flow rate was used for all succeeding studies. A series of experiments was carried out over a range of temperatures between 1256 and 1410°C, using nitrogen and then 95% nitrogen–5% hydrogen, to establish the relative merits of the two nitriding gases. Extents of nitridation, expressed as f_N, as a function of time are shown in Fig. 4 for nitrogen and Fig. 5 for nitrogen–hydrogen. Nitrogen–hydrogen gave significant improvements in yield and was subsequently used as the nitriding gas for all further experiments. The results of a series of nitridations using 95% nitrogen–5% hydrogen at temperatures of 1260–1500°C are shown in Fig. 6, which indicates that the maximum temperature for silicon nitride formation was ~ 1425°C. At this temperature, the reaction is nearly complete in ~ 7 ks. In order to show more effectively the possible effects of various additives, subsequent kinetic studies were carried out at the slightly lower than optimum temperature of 1400°C. Semilogarithmic plots of the effects of a range of additives on nitridation at 1400°C for a time of 7 ks, are shown in Fig. 7(a) and (b). Figure 7(c) shows a graph corrected to allow for TiN and CeN formation. Figures 8 and 9 illustrate the effect of temperature on the nitridation of PRH powder with additions of iron (III) oxide and nickel (II) oxide respectively. Table 3 summarizes the phase composition of the product of nitridation at 1400°C for 7 ks.

Table 2. Chemical composition of rice husk ash after washing with 0·3 M HCl

Constituent	*Mass %*
SiO_2	97·58
Al_2O_3	0·13
CaO	0·03
Fe_2O_3	0·03
MgO	0·04
K_2O	0·15
Na_2O	0·06
Ignition loss	2·27

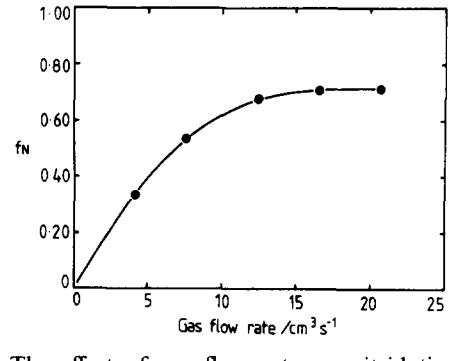

Fig. 3. The effect of gas flow rate on nitridation of PRH powder at 1400°C for a time of 7 ks in 95% nitrogen–5% hydrogen.

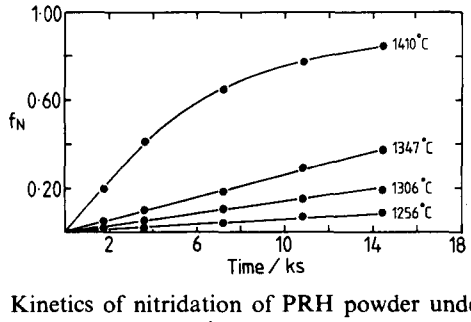

Fig. 4. Kinetics of nitridation of PRH powder under 100% nitrogen.

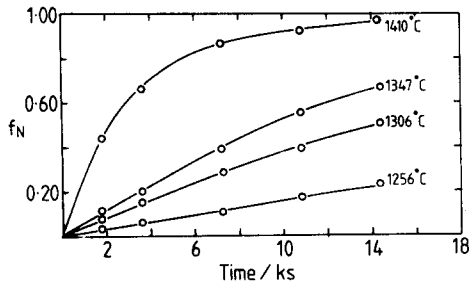

Fig. 5. Kinetics of nitridation of PRH powder under 95% nitrogen–5% hydrogen.

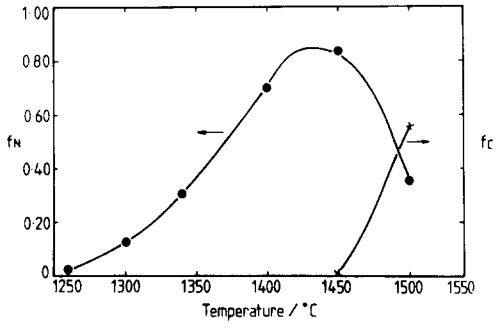

Fig. 6. The effect of temperature on nitridation of PRH powder for a time of 7 ks in 95% nitrogen–5% hydrogen.

Table 4 shows the variation of tap density of the PRH powder with particle size range, and the subsequent results on the nitridation of PRH powder at 1400°C for 7 ks. Scanning electron micrographs of the subsequent silicon nitride powder are shown in Fig. 10. Coarse powder with a particle size $>350\,\mu m$ gave predominantly α-phase material in whisker form. The proportion of whisker material present decreased as the PRH particle size decreased. With PRH powder of $\leq 53\,\mu m$, practically no whiskers were observed. The product

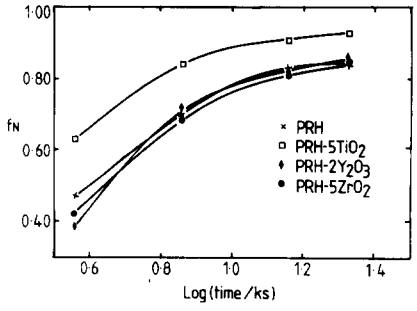

(a)

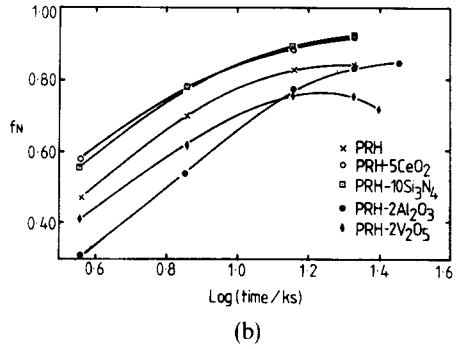

(b)

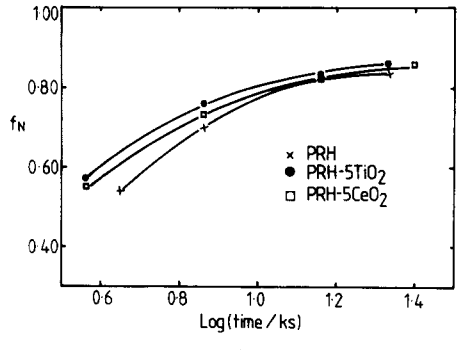

(c)

Fig. 7. (a) and (b) Semilogarithmic treatment of the effects of different materials incorporated into PRH powder on nitridation at 1400°C in 95% nitrogen–5% hydrogen; (c) the curves corrected for the formation of TiN and CeN.

Table 3. Phase detected by XRD analysis of nitrided products at 1400°C for 7 ks in 95% nitrogen–5% hydrogen

Sample	*α-Si_3N_4*	*β-Si_3N_4*	*Phase content (mass %)*		
			Si_2N_2O	*SiC*	*Other*
Standard					
PRH	99	1	—	—	—
Group 1					
PRH–$2Al_2O_3$	93	5·0	2	—	mullite (trace)
PRH–$2Y_2O_3$	98	2	trace	—	$Y_2Si_2O_7$
PRH–$5ZrO_2$	99	1	trace	—	ZrO_2
Group 2					
PRH–$5TiO_2$	99	1	trace	—	TiN
PRH–$5CeO_2$	93	3	3	—	CeN
Group 3					
PRH–$2Fe_2O_3$	60	9	trace	30	Fe_3Si, $FeSi_2$ (trace)
PRH–2NiO	45	14	—	41	Ni_3Si, $NiSi_2$ (trace)
Group 4					
PRH–$2V_2O_5$	29	71	—	—	V_2O_5 (trace)
Seed					
PRH–$10Si_3N_4$	99	1	—	—	—

Table 4. Variation of tap density with PRH particle size range and the effect of nitridation at 1400°C for 7 ks under 95% nitrogen–5% hydrogen

Particle size (μm)	*Tap density* ($kg\ m^{-3}$)	f_N
>350	230	0·73
350–210	300	0·74
210–53	340	0·73
≤53	600	0·74

silicon nitride consisted of hexagonal cross-section columnar α-phase grains.

Figure 11(a) shows examples of silicon nitride powder prepared from PRH–$2V_2O_5$ at 1400°C, and Fig. 11(b)–(c) and (d) are powder from PRH–$2Fe_2O_3$ and PRH–2NiO, respectively, after nitridation for 7 ks at 1500°C. Figure 11(a) shows a microstructure consisting of both fine and fibrous (1–2 μm length) β-silicon nitride. Some globules at the tips of whiskers were observed in silicon nitride prepared from PRH–$2Fe_2O_3$ and PRH–2NiO (Fig. 11(c) and 11(d)). EDAX analyses showed that the globules in Fig. 11(c) contained iron and silicon, while those in Fig. 11(d) contained nickel and silicon. The morphology of silicon nitride powder obtained in the presence of other metal oxides consists of hexagonal cross-section columnar grains, similar to those of the standard PRH.

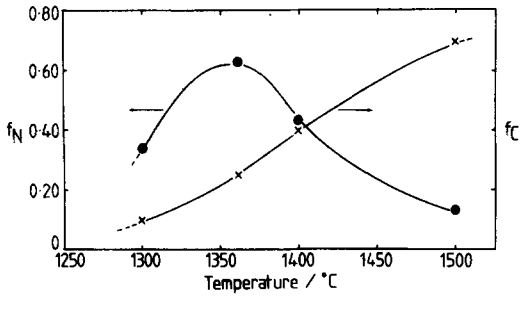

Fig. 8. Effect of temperature on nitridation of PRH–$2Fe_2O_3$ in 95% nitrogen–5% hydrogen for a time of 7 ks.

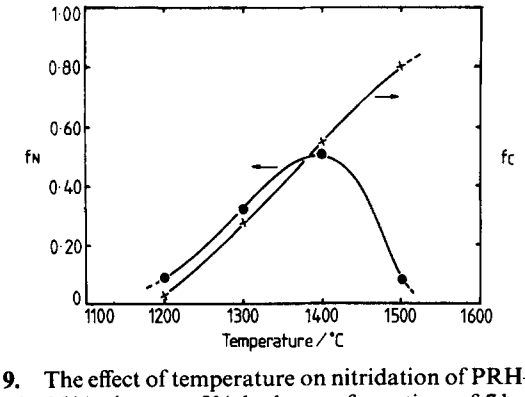

Fig. 9. The effect of temperature on nitridation of PRH–2NiO in 95% nitrogen–5% hydrogen for a time of 7 ks.

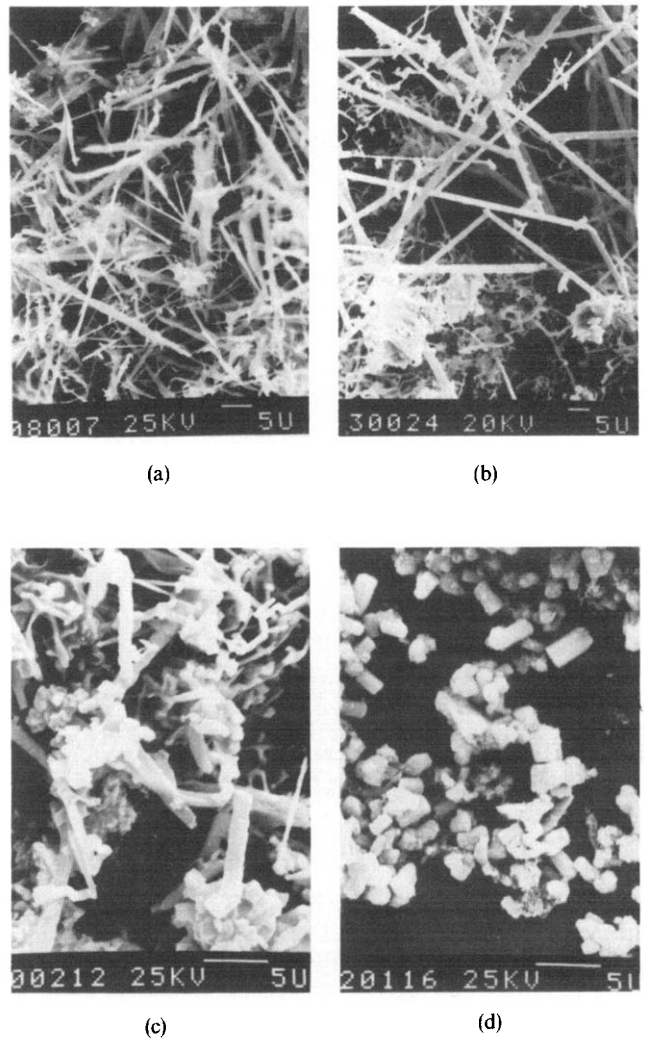

Fig. 10. SEM of powder obtained from nitridation of different particle size ranges of PRH powder at 1400°C for 7 ks in 95% nitrogen–5% hydrogen. (a) >350 μm; (b) 350–210 μm; (c) 210–53 μm; (d) ≤53 μm.

Nitridations of PRH powders milled for 90 s and 1·8 ks, and after milling for 90 s with the addition of 10 mass % silicon nitride (PRH–$10Si_3N_4$), were carried out at 1425°C for a time of 60 ks. Scanning electron micrographs of the nitrided products are shown in Fig. 12, and Table 5 lists some characteristics of these silicon nitride powders.

4 Discussion

4.1 PRH nitridation

This study has shown that three factors have a marked influence on the rate of conversion of silicon dioxide to silicon nitride: the gas flow rate, the presence of hydrogen, and the presence of preformed silicon nitride in the system. The overall

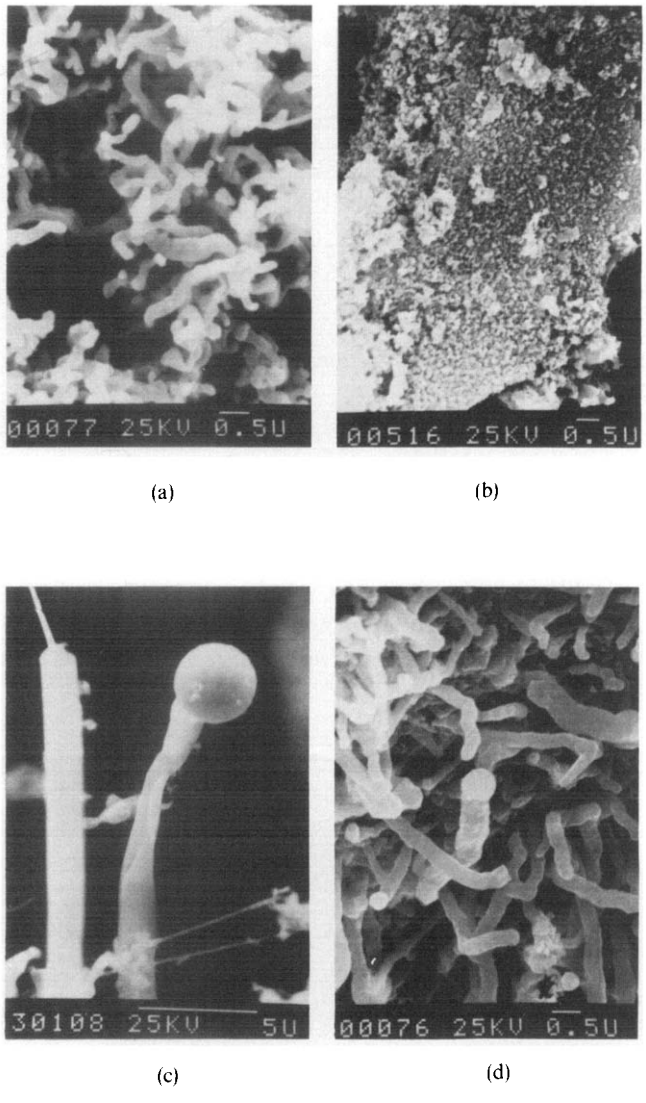

(a) (b)

(c) (d)

Fig. 11. SEM of powder obtained from nitridation of (a) PRH–V_2O_5 at 1400°C, (b) and (c) PRH–$2Fe_2O_3$ and (d) PRH–2NiO at 1500°C for 7 ks in 95% nitrogen–5% hydrogen.

reduction reaction is best depicted as occurring in two steps, a preliminary reduction stage:

$$SiO_{2(s)} + C_{(s)} \rightarrow SiO_{(g)} + CO_{(g)}$$
$$\Delta G^{\circ}_{1700K} = 107\,kJ\,mol^{-1} \quad (2a)$$

or

$$SiO_{2(s)} + H_{2(g)} \rightarrow SiO_{(g)} + H_2O_{(g)}$$
$$\Delta G^{\circ}_{1700K} = 214\,kJ\,mol^{-1} \quad (2b)$$

followed by reaction of silicon monoxide to form silicon nitride:

$$SiO_{(g)} + \tfrac{2}{3}N_{2(g)} \rightarrow \tfrac{1}{3}Si_3N_{4(s)} + \tfrac{1}{2}O_{2(g)}$$
$$\Delta G^{\circ}_{1700K} = 182\,kJ\,mol^{-1} \quad (3)$$

The free energy data are obtained from Ref. 19. The oxygen released by reaction (3) is presumably effectively scavenged by reaction with carbon or hydrogen:

$$\tfrac{1}{2}O_{2(g)} + C_{(s)} = CO_{(g)}$$
$$\Delta G^{\circ}_{1700K} = -261\,kJ\,mol^{-1} \quad (4)$$
$$\tfrac{1}{2}O_{2(g)} + H_{2(g)} = H_2O_{(g)}$$
$$\Delta G^{\circ}_{1700K} = -153\,kJ\,mol^{-1} \quad (5)$$

It is theoretically possible also for carbon monoxide to react with silicon dioxide to produce silicon monoxide:

$$SiO_{2(s)} + CO_{(g)} = SiO_{(g)} + CO_{2(g)}$$
$$\Delta G^{\circ}_{1700K} = 232\,kJ\,mol^{-1} \quad (6)$$

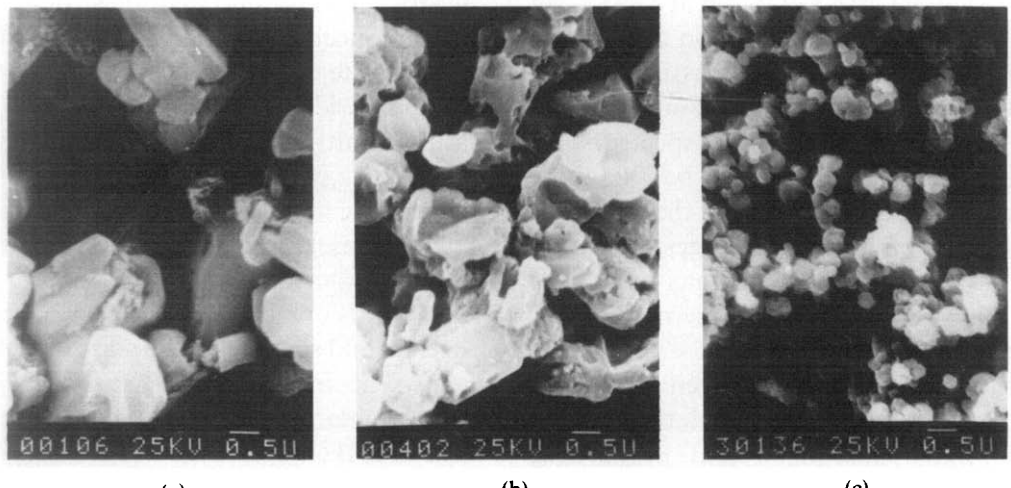

(a) (b) (c)

Fig. 12. SEM of powder obtained from nitridation of PRH powder with different milling times: (a) 90 s, (b) 1·8 ks, and (c) 90 s + 10 mass % Si_3N_4 at 1425°C for a time of 60 ks in 95% nitrogen–5% hydrogen.

Table 5. Some characteristics of silicon nitride powders prepared by nitridation of PRH powders

	PRH milling times		
	90 *s*	1·8 *ks*	90 *s* + 10 *mass* % Si_3N_4
Specific surface area ($m^2\ g^{-1}$)	2·9	4·2	6·4
Nitrogen fraction (f_N)	0·94	0·93	0·95
Residual carbon (mass %)	1·3	1·0	0·3
Silicon dioxide (mass %)	4·8	6·1	4·5
Metallic oxides total[a] (Fe_2O_3, Al_2O_3, CaO, MgO) (mass %)	0·3	0·3	0·3

[a] Estimated from the composition of the ash by assuming that potassium and sodium oxides are volatile at 1500°C.

The influence of gas flow rate on nitridation rate (Fig. 3) indicating that purging of carbon monoxide from the system is essential for nitridation to proceed, provides evidence that reaction (6) will, however, probably not make a significant contribution to silicon monoxide yield. Supporting evidence is provided by the observations of Higgins and Hendry,[20] that the presence of even a small amount of carbon monoxide in a nitriding atmosphere appears to have a marked inhibiting effect in a closely similar system (the formation of β'-sialon from mixed kaolinite and carbon powder). It is seen from Fig. 3 that in the present system, at nitrogen flow rates of $17\,cm^3\,s^{-1}$ and above, the partial pressure of carbon monoxide appears to be kept adequately low; the rate of the forward reaction (2a) is thus controlling, and the rate of formation of silicon nitride is independent of gas flow rate. This is consistent with the measurements of Van Dijen *et al.*,[21] who, using packed powder beds, also found a critical flow rate of $\sim 17\,cm^3\,s^{-1}$ at 1400°C, above which gas diffusion was no longer rate controlling.

The equilibrium pressure of silicon monoxide generated by reaction (2a) is 0·023 atm at 1700 K, on the basis of the simplifying assumption that locally $p_{CO} = p_{SiO}$. From reaction (2b) and assuming that $p_{H_2O} = p_{SiO}$, and $p_{H_2} = 0{\cdot}05$ atm, a silicon monoxide partial pressure of 1×10^{-4} atm is expected. This would suggest that carbon should be the more effective reducing species. However, the observed accelerating action of hydrogen suggests that the mobility of the hydrogen molecule may be able to compensate to a large extent for the thermodynamic disadvantages.

The equilibrium pressure of oxygen associated with reaction (3) may be calculated to be $3{\cdot}3 \times 10^{-15}$ atm; subsequent, and presumably fast, reaction of the oxygen through reaction (4) or (5) is needed to permit the nitridation reaction to proceed. This is not likely to present any problem. For example, at 1700 K reaction (4) has $kp = p_{CO}/(p_{O_2})^{1/2} = 1{\cdot}0 \times 10^8$, giving a theoretical equilibrium pressure of carbon monoxide of 6 atm.

The silicon nitride formation process may therefore be modelled on the basis of the reaction sequences:

$$SiO_{2(s)} + C_{(s)} \underset{k_2\ \text{fast}}{\overset{k_1\ \text{slow}}{\rightleftharpoons}} SiO_{(g)} + CO_{(g)} \qquad (2a)$$

$$SiO_{2(s)} + H_{2(g)} \underset{k_4\ \text{fast}}{\overset{k_3\ \text{slow}}{\rightleftharpoons}} SiO_{(g)} + H_2O_{(g)} \qquad (2b)$$

$$SiO_{(g)} + \tfrac{2}{3}N_{2(g)} \overset{k_5\ \text{slow}}{\rightarrow} \tfrac{1}{3}Si_3N_{4(s)} + \tfrac{1}{2}O_{2(g)} \qquad (3)$$

$$\tfrac{1}{2}O_{2(g)} + C_{(s)} \overset{k_6\ \text{fast}}{\rightarrow} CO_{(g)} \qquad (4)$$

$$\tfrac{1}{2}O_{2(g)} + H_{2(g)} \overset{k_7\ \text{fast}}{\rightarrow} H_2O_{(g)} \qquad (5)$$

The overall silicon nitride formation rate ($\dot{f}_N$) is thus given by

$$\dot{f}_N = a S k_5 p_{SiO} p_{N_2}$$

where a is a constant and the term S is proportional to the concentration of reaction sites. The increase in growth site density by incorporation of pre-formed silicon nitride powder provides the expected acceleration of nitride production rate (Section 4.2.2). The value of p_{SiO} appears to be the critical factor, in that it is sensitive to the local pressure of carbon monoxide.

The present programme has been concerned with 'naturally' mixed carbon and silicon dioxide molecular units or particles, rather than artificially milled carbon and silicon dioxide starting powders. Table 4 shows no increase in the extent of nitridation of PRH (under standardized conditions) as the particle size of PRH is decreased by a factor of 7. This is quite different from earlier results[10,11] concerned with the nitridation of carbon–silicon dioxide mixtures and where the silicon nitride formation rate increased

approximately linearly with decreasing reactant particle size. However, an increase in surface area should lead to enhancement of the rate of reaction (2a). It seems likely therefore that the PRH material has a large internal surface area, and that the effective reaction surface is not changed detectably by the milling treatment used here. Attempts to measure the specific surface area of PRH using a standard BET method were unsuccessful because of problems encountered with the prolonged outgassing of samples on warming from liquid nitrogen temperature. The specific surface area seemed likely to be very large.

The observed activation enthalpies for the formation of silicon nitride in nitrogen, and in nitrogen–hydrogen, are $400\,kJ\,mol^{-1}$ and $320\,kJ\,mol^{-1}$, respectively. Assuming processes (2a) and (2b) to be additive allows the value of $350\,kJ\,mol^{-1}$ to be calculated for the action of hydrogen in the absence of carbon. Accepted values for the oxygen bond strengths of C≡O and H—O are $1070\,kJ\,mol^{-1}$ and $464\,kJ\,mol^{-1}$, respectively.[22] The bond strength difference between C≡O and 2H—O ($928\,kJ\,mol^{-1}$) is thus ~13%. This is also the observed difference between the activation enthalpies for silicon nitride formation involving carbon (reaction (2a)) and hydrogen (reaction (2b)). This agreement must be fortuitous because these enthalpies are certainly composite figures containing at least two terms. It is, however, clearly unlikely that the two reaction sequences differing only in the choice of one stage ((2a) or (2b)) will have significantly different overall enthalpies, consistent with the above observation.

Although no kinetic differences are detected on the nitridation of PRH powder of different particle size ranges, there is a close relationship between PRH particle size and the morphology of the resulting silicon nitride (Fig. 10). The growth of whiskers appears to be favoured by a high compact void content, indicated by the lower tap densities of the coarser PRH powders. The finer PRH powders pack better and yield smaller, hexagonal cross-section columnar silicon nitride grains of axial ratio ~2. A possible explanation for this is that the smaller PRH particles provide a higher density of nucleation sites for silicon nitride growth. That the morphology of the silicon nitride particles is always completely different from morphology of the reaction PRH particles confirms that the silicon nitride formation reaction involves only vapour phase species reacting initially at small nuclei. In all cases α-Si_3N_4 is the major product phase, consistent with the view that formation of this phase takes place by a vapour phase reaction.[5–11]

The extent of silicon nitride formation under standard conditions increases rapidly with temperature up to a maximum at ~1425°C, above which a decrease is seen (Fig. 6). At 1450°C and above silicon carbide formation becomes significant due to the high temperature instability of silicon nitride in the presence of carbon:

$$Si_3N_{4(s)} + 3C_{(s)} = SiC_{(s)} + 2N_{2(g)}$$
$$\Delta G^{\circ}_{1723\,K} = -3\,kJ\,mol^{-1} \quad (7)$$

At 1723 K (1450°C), $kp = 1{\cdot}2$, and $p_{N_2} = 1{\cdot}1$ atm. Thus, the experimental boundary temperature between silicon nitride and silicon carbide stability is ~1450°C, in agreement with Komeya and Inoue.[5]

4.2 Effect of additives

4.2.1 Metal oxides

The behaviour of metal oxides incorporated into PRH before nitridation falls into four distinct categories, which can be interpreted in the light of the likely chemical reactivity of the metal oxide (Figs 13 and 14). No evidence was obtained for any marked catalytic action of these metal oxides on the nitridation. The presence of hydrogen in the system will not alter the overall pattern of behaviour. Both figures highlight the necessity for the effective purging of CO and H_2O from the nitridation system.

(1) Y_2O_3 and ZrO_2 are not significantly reduced by carbon or hydrogen under nitridation conditions and are without effect on the amount of silicon nitride formed. Figure 13 suggests that reduction and nitridation of

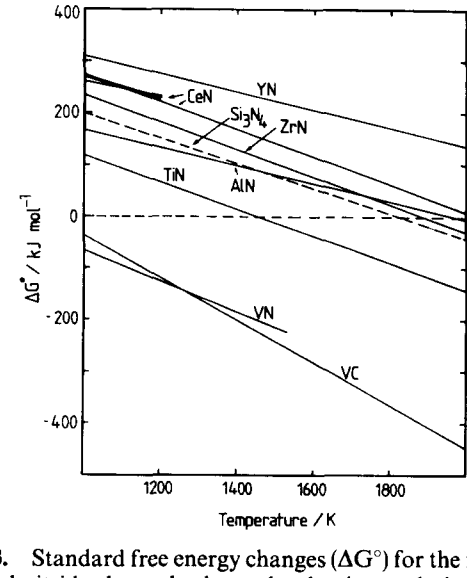

Fig. 13. Standard free energy changes (ΔG°) for the formation of metal nitrides by carbothermal reduction and nitridation of oxides: $MO_{(s)} + \frac{1}{2}N_{2(g)} + C_{(s)} \rightarrow MN_{(s)} + CO_{(g)}$; ΔG° per mole of nitride.

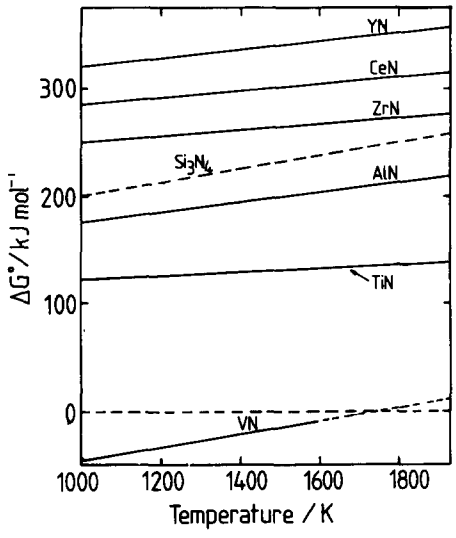

Fig. 14. Standard free energy changes (ΔG°) for the formation of metal nitrides in hydrogen atmosphere; ΔG° per mole of nitride.

ZrO_2 might occur, but XRD analyses show that ZrO_2 remained as the oxide in the silicon nitride product (Table 3). Y_2O_3 reacted to some extent with SiO_2 to form $Y_2Si_2O_7$ which could be detected subsequently by XRD. Al_2O_3 is unstable under the reduction conditions and reacts in the presence of SiO_2 to yield β'-sialon.[20] In the present case the extent of nitride formation appears to be diminished in the earliest stages of the nitridation (< 15 ks), although the later reaction rates are not different from those of PRH alone. The initial retarding action of Al_2O_3 may be related to the formation of mullite, which was detected by XRD, and to the relative difficulty of nitriding mullite in comparison with the more finely mixed silicon dioxide–carbon of the PRH. Al_2O_3 appears to favour the formation of β-phase silicon nitride, but in fact this is certainly a β'-sialon.

(2) Both TiO_2 and CeO_2 appeared to accelerate silicon nitride formation, and led to higher overall yields. This is only apparent; TiO_2 is readily reduced and nitrided (reaction (8)) and the final nitrogen analysis is not able to distinguish between TiN and Si_3N_4.

$$2TiO_{2(s)} + 4C_{(s)} + N_{2(g)} \rightarrow 2TiN_{(s)} + 4CO_{(g)} \quad (8)$$

CeO_2 is also readily reduced to Ce_2O_3, with a range of intermediate non-stoichiometric oxides CeO_{2-x}. Thermodynamic data are available only to 1200 K and extrapolations cannot therefore be made with reliability. XRD evidence was obtained, however, for the presence of CeN in the silicon nitride, which is assumed to account for the higher nitrogen content observed. The reason for the discrepancy between observation and theory in the CeN case is thus likely to be the result of the departure in the reacting system from true thermodynamic equilibrium. The nitride yield curves, corrected for the formation of TiN and CeN, are shown in Fig. 7(c) and give no evidence for any accelerating action of either TiO_2 or CeO_2.

(3) Fe_2O_3 and NiO are readily reduced under low oxygen partial pressure to the metals, which in turn yield the liquid silicides at the nitridation temperature. The nitridation of Fe_2O_3–PRH resulted in the production of a mixture of SiC and Si_3N_4. Globules at whisker tips are seen, indicative of a vapour–liquid–solid (VLS) mechanism of growth.[23] Although the exact composition of the globules could not be determined by EDAX, the presence of iron was established, and the iron silicides Fe_3Si and $FeSi_2$ were detected by XRD. The SiC thus partly grows at the liquid–solid interface through solution into the liquid of SiO and CO.[23]

$$SiO_{(g)} + 2CO_{(g)} \rightarrow SiC_{(s)} + CO_{2(g)} \quad (9)$$

Most of the silicon carbide, however, appears to be formed by the reaction of SiO with carbon (reaction 10), as evidenced by the part-retention of the PRH structure in the silicon carbide (Fig. 11(b)).

$$SiO_{(g)} + C_{(s)} \rightarrow SiC_{(s)} + CO_{(g)} \quad (10)$$

Figure 8 appears to indicate a maximum in the nitrogen fraction (f_N) of ~0·65 at ~1350°C after 7 ks, although a significant amount of SiC was also formed ($f_C \sim 0{\cdot}25$). Hanna *et al.*[14] observed that the maximum yield of Si_3N_4 was obtained at 1300°C with 7 mass % Fe, and with no appearance of silicon carbide. These authors also concluded that the presence of iron was essential for the production of silicon nitride at temperatures below 1500°C. In contrast, the present study shows that silicon nitride may be formed readily at temperatures up to 1425°C in the absence of iron, and indeed that iron is undesirable in that it tends to lead to contamination by silicon carbide.

Figure 9 shows that NiO is similarly very effective at catalysing the formation of silicon

carbide. EDAX and XRD analyses confirmed the presence of nickel silicides in the metallic globules.

(4) V_2O_5 melts at 690°C, and was found to be effective in generating the β-Si_3N_4 phase (Table 3). In view of the possibility that V^{3+} (and O^{2-}) might have been incorporated in the Si_3N_4 lattice to form a β'-sialon type solid solution, careful *d*-spacing measurements were made, but no shifts from the expected β-Si_3N_4 values were detected. The formation of solid solutions thus appears to be unlikely, and the most probable explanation is that the growth of β-Si_3N_4 is favoured by the presence of liquid V_2O_5, as it is by other liquids[24] in the absence of carbon. That silicon carbide growth also is not favoured by the presence of this liquid may mean either that only metallic liquids are effective in this respect, or that the V_2O_5 itself acts as a competitive sink for carbon by reaction (11). VC and VN were both detected by XRD in the nitrided PRH–$2V_2O_5$.

$$V_2O_{5(s)} + 7C_{(s)} \rightarrow 2VC_{(s)} + 5CO_{(g)} \quad (11)$$

After burn-off of the excess carbon according to the standard procedure, V_2O_5 soluble in sodium hydroxide solution remained. The apparently low overall yield of silicon nitride in the presence of V_2O_5 may be attributable in part to a higher than normal oxidation rate of the whiskery, high surface area, β-Si_3N_4 (Fig. 11(a)) during carbon burn-off or simply to a reduction in the rate of the α-Si_3N_4-forming reaction (3).

4.2.2. Silicon nitride

Even with the finely milled PRH, silicon nitride grains of aspect ratio ~1 were produced (Fig. 10(d)). This contrasts markedly with the fibrous silicon nitride produced from roughly crushed PRH, and with that reported by Hanna *et al.*[14] High packing density α-Si_3N_4 powder with equiaxed grains of particle size $<0{\cdot}5\,\mu$m would be preferable as a starting material for the production of sintered silicon nitride. Milling PRH for 2 ks yielded silicon nitride of increased specific surface area, with hexagonal symmetry particles that were slightly irregular and distorted. Closer examination by SEM of material after carbon burn-off showed that the crystal surfaces were rough and contained surface porosity (Fig. 12(b)). This feature, which may be due to the loss of entrapped excess particulate carbon, seems likely to account in large measure for the increase in specific surface area observed (Table 5). The effect of milling the PRH on the silicon nitride crystal size is seen as that of an increased nucleation site density for the growth of α-Si_3N_4. Similar effects have been reported by Inoue *et al.*[6] and Zhang & Cannon.[9] Additional nuclei were therefore introduced into PRH powder through the use of a high specific surface area commercial silicon nitride powder. Figure 12(c) shows that the nitrided product now consists of equiaxed silicon nitride grains with an increase in the specific surface area by a factor of ~1·5. Kinetic studies at 1400°C (Fig. 7(b)) show also an improved yield (f_N) of silicon nitride (~10%), and a significant reduction of ~80% in the amount of the residual carbon (Table 5). These observations support the view that the most effective growth sites for silicon nitride are the silicon nitride grains themselves, and not the PRH particles. The partial pressure of nitrogen associated with reaction (7) at 1700 K is 0·85 atm lower than the experimental nitrogen pressure at 0·95 atm. Thus, silicon nitride seeds will be stable and provide growth site for secondary silicon nitride. The small amount of residual carbon in this form of silicon nitride powder is readily burned off, leaving a very small residue of trapped carbon (~0·3 mass %) within the silicon nitride grain. Silicon nitride powder was subsequently produced under these conditions in larger quantities for further investigation of its sintering densification behaviour.

5 Conclusions

Silicon nitride of a high degree of chemical purity and predominantly of the α-phase can be obtained through the carbothermal nitridation of pyrolysed rice husk powder at temperatures in the range 1260–1450°C under 95% nitrogen–5% hydrogen. Hydrogen addition is beneficial in accelerating the nitride formation rate. The boundary temperature between silicon nitride and silicon carbide formation is ~1450°C.

The morphology of the silicon nitride powder depends critically on the growth nuclei density. The addition of pre-formed silicon nitride powder to PRH powder before nitridation is markedly beneficial in yielding a product consisting of uniform sub-micrometer ($<0{\cdot}5\,\mu$m), equiaxed, α-Si_3N_4 crystals. A search for catalysts of the metal oxide type able to accelerate the nitridation rate failed; a small increase in reaction rate was observed with the addition of pre-formed silicon nitride. The effectiveness of the PRH as a source of silicon nitride is seen

to be associated closely with the material's structure and composition, and the intimate mixing obtained for the silicon dioxide and carbon. Rice husk is thus potentially a cheap, readily available raw material for high purity, controlled morphology, sinterable silicon nitride powder.

Acknowledgements

The financial support of the University of Science, Penang, and the Malaysian Government for this programme in the form of a Studentship, is gratefully acknowledged. The University of Science, Penang, is thanked for the supply of rice husk.

References

1. Vanedenede, V., Leriche, A., Cambier, F., Pickup, H. & Brook, R. J., Sinterability of silicon nitride powders and characterization of sintered material. In *Non-oxide Technical and Engineering Ceramics*, ed. S. Hampshire. Elsevier, London, 1986, pp. 53–67.
2. Lange, F. F., Silicon nitride polyphase systems: Fabrication, microstructure and properties. *Int. Metal. Rev.*, No. 1 (1980) 1–20.
3. Hendry, A. & Jack, K. H., The preparation of silicon nitride from silica. In *Special Ceramic—6*, ed. P. Popper. British Ceramic Research Association, Stoke-on-Trent, 1975, pp. 199–205.
4. Lee, J. G. & Cutler, I. B., Reactions in the SiO_2–C–N_2 system. In *Nitrogen Ceramics*, ed. F. L. Riley. Noordhoff, Leyden, 1977, pp. 175–81.
5. Komeya, K. & Inoue, H., Synthesis of the α-form of silicon nitride from silica. *J. Mat. Sci. Letters*, **10** (1975) 1243–6.
6. Inoue, H., Komeya, K. & Tsuge, A., Synthesis of silicon nitride powder from silica reduction. *Comm. Am. Ceram. Soc.*, (1982) C205.
7. Mori, M., Inoue, H. & Ochiai, T., Preparation of silicon nitride powder from silica. In *Progress in Nitrogen Ceramics*, ed. F. L. Riley. Martinus Nijhoff, The Hague, 1983, pp. 149–55.
8. Lee, J. G., Carbide and nitride ceramics by carbothermal reduction of silica. PhD Thesis, University of Utah, 1975.
9. Zhang, S. C. & Cannon, W. R., Preparation of silicon nitride from silica. *J. Am. Ceram. Soc.*, **67**(10) (1985) 691–5.
10. Houston, D. F., *Rice Chemistry and Technology*. American Association of Cereal Chemistry Inc., St. Paul, MN, 1972, pp. 301–52.
11. Lee, J. G. & Cutler, I. B., Formation of silicon carbide from rice hulls. *Am. Ceram. Bull.*, **54**(2) (1975) 195–8.
12. Mansour, N. A. L. & Hanna, S. B., Silicon carbide and nitride from rice hulls—II: Effect of iron on the formation of silicon carbide. *Brit. Ceram. Soc. Trans. J.*, **68**(6) (1979) 132–6.
13. Sharma, N. K. & Williams, W. S., Formation and structure of silicon carbide whiskers from rice husk. *J. Am. Ceram. Soc.*, **67**(11) (1984) 715–20.
14. Hanna, S. B., Mansour, N. A. L., Taha, A. S. & Abd Allah, H. M. S., Silicon carbide and nitride from rice hulls—III: Formation of silicon nitride. *Brit. Ceram. Trans. J.*, **84**(1) (1985) 18–21.
15. Kang, S. W. & Chun, S., The kinetics of Si_3N_4 formation from Korean rice hulls. *J. Korean Ceram. Soc.*, **16**(2) (1979) 99–104.
16. Siddiqi, S. A. & Hendry, A., Influence of iron on the preparation of silicon nitride from silica. *J. Mater. Sci.*, **20** (1985) 3230–8.
17. Tasser, R. G., Hart, A. & Julietti, R. J., A rapid method for determining nitrogen in nitrides. *Analyst*, **87** (1962) 501–2.
18. Weston, R. J., The kinetics and mechanism of the hot-pressing of silicon nitride. PhD Thesis, University of Leeds, 1976.
19. Barin I. & Knacke, O., *Thermodynamic Properties of Inorganic Substances*. Springer-Verlag, Berlin, 1973.
20. Higgins, I. & Hendry, A., Production of β'-sialon by carbothermal reduction of clay. *Brit. Ceram. Soc. Trans. J.*, **85**(5) (1986) 161–6.
21. Van Dijen, F. K., Metselaar, R. & Siskens, C. A. M., Reaction-rate limiting steps in carbothermal reduction processes. *J. Am. Ceram. Soc.*, **68**(1) (1985) 16–19.
22. Masterton, W. L., Slowinski, E. J. & Stanitski, C. L., *Chemical Principles*, 6th edn. CBS College, USA, 1985, p. 281.
23. Mileweski, J. V., Gac, F. D., Petrovic, J. J. & Skaggs, S. R., Growth of beta-silicon nitride whiskers by the VLS process. *J. Mater. Sci.*, **20** (1985) 1160–6.
24. Campos-Loriz, D. & Riley, F. L., Factors affecting the formation of the α- and β-phases of silicon nitride in the nitridation of silicon powder. *Science of Ceramics*, **9** (1975) 38–45.